Characterization of SCaMC-3-Like/slc25a41 a novel calcium-independent mitochondrial ATP-Mg/Pi carrier

Javier Traba, Jorgina Satrústegui, Araceli del Arco

Characterization of SCaMC-3-Like/slc25a41 a novel calcium-independent mitochondrial ATP-Mg/Pi carrier

Javier Traba[*], **Jorgina Satrústegui**[*] **and Araceli del Arco**[*,†]

† Área de Bioquímica, Centro Regional de Investigaciones Biomédicas (CRIB), Facultad de Ciencias del Medio Ambiente, Universidad de Castilla-La Mancha, Toledo, Spain.
*Departamento de Biología Molecular, Centro de Biología Molecular Severo Ochoa UAM-CSIC, Universidad Autónoma, CIBER de Enfermedades Raras (CIBERER), Madrid, Spain;

† **Correspondence:** Araceli del Arco, Facultad de Ciencias del Medio Ambiente, Campus Tecnológico de la Antigua Fábrica de Armas, Avda. Carlos III s/n, Toledo, 48071, Spain
Tel: 034-911964651; Fax: 034-911964420; E-mail: Araceli.Arco@uclm.es

Short title: A novel Ca^{2+}-independent ATP-Mg/Pi carrier

Keywords: SCaMC, mitochondrial carrier, gene duplication, mitochondrial ATP

Abbreviations: CAT, carboxyatractyloside; SCaMCs, Short Calcium-Binding Mitochondrial Carriers; BtAAC1, ADP/ATP carrier 1 from *Bos taurus*; MCs, mitochondrial carriers; mtDNA: mitochondrial DNA; MCF, mitochondrial carrier family.

SYNOPSIS

The SCaMCs constitute a subfamily of mitochondrial carriers responsible of the ATP-Mg/Pi exchange with at least three paralogues in vertebrates. SCaMCs members are proteins with two functional domains the C-terminal transporter domain and the N-terminal one which harbours Ca^{2+}-binding EF-hands and facing the intermembrane space. Here, we have characterised a shortened fourth paralog, SCaMC-3-Like (also named as Slc25a41), which lacks the Ca^{2+}-binding N-extension. SCaMC-3-Like orthologues are found exclusively in mammals showing around 60% identity to the carboxyl-half of SCaMC-3, its closest paralog. In mammalian genomes, *SCaMC-3* and *SCaMC-3-Like* genes are adjacent on the same chromosome, forming a head-to-tail tandem array and show identical exon-intron boundaries indicating that *SCaMC-3-Like* could have arisen from a *SCaMC-3* ancestor by a partial duplication event which occurred prior to mammalian radiation. Expression and functional data suggest that following the duplication event, *SCaMC-3-Like* has acquired more restrictive functions. Unlike the broadly expressed longer SCaMCs, mouse *SCaMC-3-Like* shows a limited expression pattern; it is preferentially expressed in testis and, at lower levels, in brain. SCaMC-3-Like transport activity was studied in yeast deficient in Sal1p, the Ca^{2+}-dependent mitochondrial ATP-Mg/Pi carrier, co-expressing SCaMC-3-Like and mitochondrial-targeted luciferase, and it was found to perform ATP-Mg/Pi exchange, as Sal1p or other ATP-Mg/Pi carriers. However, metabolite transport through SCaMC-3-Like is Ca^{2+}-independent, representing a novel mechanism involved in adenine nucleotide transport across the inner mitochondrial membrane different to ADP/ATP translocases or long SCaMC paralogues.

INTRODUCTION

The transport of metabolites, nucleotides and co-factors across the inner mitochondrial membrane is performed by structurally related proteins belonging to the mitochondrial carrier family (MCF) [reviewed in 1-3]. All mitochondrial carrier members have a tripartite structure made of three repeated sequences of about 100 amino acids in length containing two transmembrane spanning segments and a characteristic sequence motif in matrix facing loops [4]. In the last years, their significant sequence conservation has permitted to characterise the repertoire of MC in numerous genomes [3, 5-9], and suggests a common ancestor in evolution [3]. Initial analysis of *S. cerevisiae* genome allowed to identify 35 MCF members [5, 9]; subsequent inspections have revealed a higher complexity in MCF from pluricellular eukaryotes and vertebrates [3, 6]. MCF complexity is mainly due to generation of paralogues and, to lesser extent, by emergence of proteins with novel transport capabilities [3]. In both processes, gene duplication has contributed as the major source for the generation of MCF functional diversity [3, 10, 11].

One of most large sub-groups of mitochondrial carriers is that formed by those involved in adenine nucleotide transport, which comprise the ADP/ATP translocases and SCaMCs (see [3], for review) with four and three paralogues characterised in mammals, respectively [3, 12, 13]. SCaMCs correspond to isoforms of the ATP-Mg/Pi carrier [12, 13]. This transport was functionally identified 20 years ago and catalyzes the net transport of adenine nucleotides across the inner mitochondrial membrane [14, 15]. It mediates a reversible electroneutral exchange between ATP-Mg^{2-} and $HP0_4^{2-}$ [13, 16]. Likewise, SCaMCs are Ca^{2+}-dependent mitochondrial carriers (CaMCs, reviewed in [17]), a subgroup of mitochondrial carriers (MC) having a bipartite structure with a C-terminal half containing the MC homology domain and a long N-terminal extension harbouring EF-hand calcium-binding motifs [12, 17-19], and whose transport activity is regulated by cytosolic Ca^{2+} [20-23]. SCaMCs complexity is increased by the existence of several spliced-variants [12, 17, 24] and the recent identification of a shortened fourth paralog, slc25a41 [25]. It has been proposed that in liver mitochondria the ATP-Mg/Pi carrier regulates the matrix adenine nucleotide content [15] contributing to the regulation of mitochondrial activities dependent on adenine nucleotides as gluconeogesis, urea synthesis or mitochondrial biogenesis [15]. In *S. cerevisiae* the mitochondrial ATP-Mg/Pi transporter, Sal1p, is recruited as a Ca^{2+}-dependent mechanism to import ATP-Mg from the citosol upon glucose addition to nutrient starved yeast. It is also involved in ATP-Mg uptake from the cytosol in yeast growing exponentially in glucose, a condition in which yeast mitochondra are ATP consumers [26, 27]. Sal1p was also involved, along with the ADP/ATP translocase Aac2p, in mitochondrial translation and mtDNA maintenance [28].

In this paper, we report a comprehensive characterization of the smaller fourth SCaMC paralog, *SCaMC-3-Like/slc25a41*, which appears to be the result of one partial tandem duplication. We show that *SCaMC-3-Like* and its closest paralog, *SCaMC-3*, display different expression patterns and genomic structure because the duplication event did not cover exons encoding the N-extension containing Ca^{2+}-binding domains. Transport assays in isolated mitochondria of yeast expressing mouse SCaMC-3-Like has confirmed that SCaMC-3-Like functions as a Ca^{2+}-independent ATP-Mg/Pi exchanger, therefore providing a novel mechanism of ATP transport across the inner mitochondrial membrane different of that described for yeast Sal1p, the liver ATP-Mg/Pi carrier and the ADP/ATP translocases.

METHODS

Searching for homologous genes and bioinformatics tools used

We have used the protein and nucleotide sequences of previously characterised human SCaMCs [12] to screen on-line genome databases (NCBI, Swiss-Prot and Ensembl) using the BLAST algorithms. Searches were carried out using default values with the low complexity filter off. TBLASTN searches were performed for genomes whose assembling and annotation process are not totally finished. Searches were performed in NCBI, and also BLAT searches in UCSC Genome Browser website (http://genome.ucsc.edu/) were occasionally performed. We used WGS assembly of the gray short-tailed opossum genome (*Monodelphis domestica*) (MonDom5) and from the monotreme platypus (*Ornithorhynchus anatinus*) (Build 1.1) (available at the NCBI). For some species whose genome annotation is still unfinished as rhesus (*Macacca mulatta*, Build 1.1) or whose protein sequences were misassembled as cow (*Bos taurus*), the identified sequences are the results of a genome-wide manual screening. Assembly of predicted sequences was undertaken using Prophet 5.0 program. Finally, sequences were aligned by ClustalW followed by manual adjustments. To distinguish among orthologues and paralogues we performed reciprocal-best-blast hit analysis. Further, orthology was verified on the basis of syntenic relationships among genes from mammalian species. Chromosomal position and orientation of duplicated pairs and their neighbouring genes was determined using NCBI Entrez GeneView. In unfinished genomes, analysis was performed on overlapping genomic clones using the TBLASTN algorithm. Analysis of repeat elements was performed in FREP (Functional Repeats) database (http://facts.gsc.riken.go.jp/FREP). SH3-Hunter program was used to find consensus signals interacting with proteins containing SH3 domains (http://cbm.bio.uniroma2.it/SH3-Hunter). Multiple sequence alignments were carried out with ClustalW program and coloured using BOXSHADE program (www.ch.embnet.org). Tree construction and bootstrap analysis were carried out with the PHYLO-WIN program [29]. We threaded the sequence of SCaMC-3L into the structure of ANT1 (PDB:1okc) [4] using the Phyre web tool (http://www.imperial.ac.uk/phyre). Secondary structure predictions were carrier out using APSSP available on the EXPASY server.

RNA isolation, RT-PCR analysis and cloning of mouse SCaMC-3-Like cDNA

Total RNA was extracted from mouse tissues by the acid guanidinium thiocyanate-phenol-chloroform procedure. First strand cDNA was synthesized by using 5 μg of total RNA from each tissue obtained as template, 100 ng of random primer (Promega), and avian myeloblastosis virus reverse transcriptase (Promega). 5 % of the yield from first strand cDNA synthesis was used as template for subsequent PCR amplifications using TaqDNA polymerase (PerkinElmer Life Sciences) under standard conditions. Specific primers derived from predicted rat LOC301114 (sense r3c-5, 5'-ACTGTGCCAGGCAGATCTTGG-3'; antisense, r3c-3, 5'-CTGCTCAGGACTTGTACACC-3'), mouse *4933406J04Rik* gene (sense m3c-5, 5'-ATGGTACCCGAGCCCTATAC-3'; antisense, m3c-3, 5'-TCTGCTCAGGACTTGTACAC-3') and mouse

SCaMC-3 (sense m3-5, 5'-TGACTCTACGCAGAACTGGC-3'; antisense, m3-3, 5'-GACCTTCATGAAGTTGGGGG-3') were used. For normalization, a pair of specific β-actin primers common for mouse and rat, sense 5'-GGTATGGAATCCTGTGGCATCCATGAAA-3' and antisense 5'-GTGTAAAACGCAGCTCAGTAACAGTCC-3', which amplify a 635-bp product, were used. The templates were amplified under the conditions described above. For β-actin levels, 28 cycles of amplification were carried out, and 35 cycles for SCaMC-3L sequences. PCR products were electrophoresed in 1.5 % agarose gels and stained with ethidium bromide. Also, the amplified products were cloned and sequenced using ABI prism dye terminator cycle sequencing kit (Applied Biosystems).

DNA constructs

The *SCaMC-3-Like* full-length cDNA was synthesized from 3 μg of total RNA of mouse testis with the Cells-to-cDNA™ II Kit (Ambion) using random primers. To obtain full-length cDNA, polymerase chain reaction was performed using specific primers. Primers were designed according to identified partial mouse EST clone BY716380 and the predicted *4933406J04Rik* gene. We have designed the following two sets of PCR primers: m3c-1/m3c-2 pair (sense, containing ATG, 5'-CAACTATGGGAGTCCATCTCG-3'and antisense 5'-TCGGTATAGGGCTCGGGTAC-3'); and the m3c-5/m3c-3 pair (sense 5'-ATGGTACCCGAGCCCTATAC-3' and antisense 5'-TCTGCTCAGGACTTGTAC-3', respectively). PCR fragments were cloned using pSTBlue1-blunt vector (Novagen) and sequenced. Finally, the whole cDNA of 941 bp (accession number FM165286) was obtained by assembling those partial sequences. Rat *SCaMC-3L* full-length cDNA (accession number FM165287) was also amplified from testis total RNA using r3c-1/r3c-2 primers (sense, 5'-CAACTATGGGAGTCCATCTGGAG-3' and antisense 5'-TCTGCTCAGGACTTGTACACC-3'). The plasmid expressing mouse SCaMC-3L-FLAG was generated by using PCR to insert DNA encoding the FLAG epitope (DYKDDDDK). FLAG-epitope was added at the COOH terminus immediately preceding the termination codon of mouse SCaMC-3L by PCR using primers m3c-1 and m3cFLAG (5'- ATCACTTGTCTACGTCGTCCTTGTAGTCTCTGCTCAGGACTTGTAC-3') containing 27 nucleotides that encode the FLAG octapeptide (underlined) following to stop codon, the resultant cDNA was cloned into pSTBlue1 and verified by sequencing. Finally, an *Eco*RI fragment containing FLAG tagged mouse SCaMC-3-Like was subcloned into expression vector pCMV5 and digested with EcoRI, to obtain pCMV5-SCaMC-3L$_{FLAG}$. To carry out expression assays in yeast, this EcoRI fragment was subcloned in EcoRI site of centromeric pYX142 plasmid (Novagen) to generate pYX142-SCaMC-3L.

Cell culture and transfection

HEK-293T and COS-7 cells were cultured in Dulbecco's modified Eagle's medium supplemented with 5 % inactivated FBS at 37 °C in a 7 % CO_2 atmosphere. Cells were grown on coverslips and transiently transfected using the LipofectAMINE reagent as described [24]. After 16-36 h of incubation to allow expression, cells were harvested for Western analysis or immunofluorescence assays. For the study of

mitochondrial location, living cells were incubated with 200 nM MitoTracker Red CMXRos (Molecular Probes) for 30 min at 37 °C or co-transfected with pDsRed2-Mito (Clontech). MitoTracker-loaded cells were fixed in 2 % paraformaldehyde (RT, 4 min) and 100 % methanol (-20 °C, 3 min), washed, and then used for immunofluorescence as described previously [12, 18]. A monoclonal antibody against FLAG peptide, clone M2 (1:100; SIGMA), was used. Fluorescence microscopy was performed using an Axioskop2 plus (Zeiss) at a nominal magnification of ×100. Digital images were taken in parallel with a Coolsnap FX camera controlled via the MetaView software.

For western blot analysis of expressed proteins, HEK-293T cells were plated in 10-cm Petri dishes and transfected with 10 μg of expression plasmids. 36 h after transfection, cells were washed and harvested by centrifugation. Mitochondria-enriched fractions were obtained as described [12]. Proteins were separated by SDS-PAGE on 10 % gels and the presence of FLAG-tagged proteins was determined by Western blotting using anti-FLAG (1:5000). Proteins were visualised by ECL (Amersham Biosciences). Polyclonal serum against human SCaMC-1 was used at 1:5000 [12].

Yeast strains and culture media

In this work we used the W303-1B wild type strain (MATα, *ura3-1*, *trp1-Δ2*, *leu2-3,112*, *his3-11*, *ade2-1*, *can1-100*) and the *sal1Δ* strain (W303; MATa, *ura3-1*, *trp1-Δ2*, *leu2-3,112*, *his3-11*, *ade2-1*, *can1-100; sal1::kanMX4*) in which *SAL1*, that codes for the mitochondrial ATP-Mg/Pi carrier, is disrupted by replacement of its complete coding sequence with the kanMX4 module [26, 27, 30]. Both contain the plasmid pYeDP-Cox4-Luciferase [27]. The *sal1Δ* strain was also transformed with plasmid pYX142 or plasmid pYX142-SCaMC-3L. For the selection of geneticine (G418; Life Technologies) resistance, cells were spread on YPD (2 % bactopeptone, 1 % yeast extract, 2 % glucose) plates containing 200 μg/mL G418 [30]. For selection of pYX142 plasmid transformants, MM (0.17 % yeast nitrogen base without amino acids and ammonium sulphate, 0.5 % ammonium sulphate, 0.2 % glucose as carbon source) plates without leucine were used. For isolation of mitochondria, yeast cells were precultured on MM (supplemented with the required appropriate auxotrophic requirements), diluted in YPGR (2 % bactopeptone, 1 % yeast extract, 2 % galactose, 2 % rafinose) and grown until late log phase.

ATP transport assays

Mitochondria were isolated as described previously [31]. Briefly, protoplasts were prepared by enzymatic digestion with zymolyase 100T (Seikagaku) and mitochondria were isolated by differential centrifugation after homogenization of protoplasts. The resuspension of final protoplast pellet and all subsequent centrifugations were performed in mitochondrial buffer**:** 0.6M mannitol, 10 mM Tris-maleate, 0.5 mM Na_2HPO_4, 0.2 % bovine serum albumin, pH 6.8 and protease inhibitors (1 mM PMSF and 1 μg/ml pepstatin A). The mitochondrial pellet was resuspended in the same medium and protein was determined by standard procedures. Assays for ATP transport were performed in 96-well microplates inside a FLUOstar OPTIMA

microplate. The luminescence signals were transformed to ATP concentration using calibration curves as described earlier [27]. The initial ATP content in freshly isolated mitochondria from *sal1Δ* cells expressing luciferase from plasmid pYeDP-Cox4-Luc and SCaMC-3L from plasmid pYX142, in our assay conditions, is 0.238 ± 0.037 nmoles ATP per mg of protein (mean ± SEM of three independent determinations; determined as in [26]), identical to that of mitochondria from W303 and *sal1Δ* cells [27], and thus the same calibration curves were used.

RESULTS AND DISCUSSION

Identification of a novel *SCaMC* paralog, *SCaMC-3-Like*, originated by a tandem duplication of a *SCaMC-3* ancestor

During the inspection of human *SCaMC-3* carboxy-variants, we detected immediately downstream of *SCaMC-3* a predicted gene, *LOC284427*, containing sequences 52-75 % identical to those of exons 5 to 10 of *SCaMC-3*. When similar analysis was performed on mouse and rat syntenic regions, equivalent counterparts, the hypothetical genes *LOC301114* and *4933406J04Rik*, were detected downstream to *SCaMC-3* genes. In addition, corresponding EST clones are also detected in mouse and human databases supporting that they are expressed genes. We have named them *SCaMC-3-Like* given that they are closely related to SCaMC-3 sequences. Recently, a partial clone corresponding to rat *LOC301114* sequences has been identified during a screening for mitochondrial carriers expressed in rat brain and numbered as *Slc25a41* [25]. In this survey, human and mouse orthologues were also identified and positioned in close proximity to their respective SCaMC-3 paralogues [25].

A detailed analysis of these loci has confirmed that all mouse, rat and human *SCaMC-3*/*SCaMC-3-Like* loci share an identical genomic organization forming a head-to-tail tandem array. A diagram of mouse genomic structure is shown in figure 1A. The predicted *SCaMC-3-Like/slc25a41* genes, hereafter *SCaMC-3L*, are composed of seven exons whereas *SCaMC-3* genes have ten exons (Fig. 1A). *SCaMC-3* and *SCaMC-3L* are separated by short intergenic regions and exon/intron boundaries of *SCaMC-3L* exons 2 to 7 perfectly match those of exons 5 to 10 of their respective *SCaMC-3* paralogues, suggesting that *SCaMC-3L* arose by a partial tandem duplication of a pre-existing *SCaMC-3* ancestor. *SCaMC-3* is most likely the ancestral locus for duplication as it contains exons absent in the shorter *SCaMC-3L*. In all *SCaMC-3L* loci analysed, sequences corresponding to *SCaMC-3* exons 1-4 encoding the Ca^{2+}-binding N-extension characteristic of the SCaMC subfamily have been lost (Fig. 1B). The predicted exons 2 to 7 of *SCaMC-3L* encode peptides highly homologous to amino acids 162 to carboxyl-end of their SCaMC-3 counterparts and a novel exon 1, *SCaMC-3*-unrelated, provides the in-frame start codon and first amino acids (see Fig. 1A). Searches using these novel exon 1 sequences fail to detect homologues belonging to other genes, implying that neighbouring sequences from its new genomic location have been probably recruited to generate this novel first *SCaMC-3L* exon.

Subsequently, we confirmed mouse and rat *SCaMC-3L* full-length coding sequences by RT-PCR with specific primers designed to anneal to predicted exons 1 and 7. The sequences obtained match well those of EST clones and encode highly conserved proteins, 95 % identical, of 312 amino acids. Mitochondrial localization of mouse SCaMC-3L was assayed in COS-7 cells by transient transfection of the full-length cDNA tagged at C-end with FLAG epitope. Cells transiently transfected with SCaMC-$3L_{FLAG}$ were later analysed by immunofluorescence with anti-FLAG antibodies. In these assays, mitochondrial localization was verified by co-staining with MitoTracker Red [18] and by co-localization with the DsRed2-Mito protein (Fig. 1C). Additionally, mitochondrial location in transfected cells was also confirmed by

subcellular fractionation and western analysis. Anti-FLAG antibodies detect a protein of the expected mass for SCaMC-3L, around 30-35 kDa, in both mitochondrial-enriched (Fig. 1D, Mit lane) and total homogenate fractions (Fig. 1D, H lane).

Interestingly, both mouse and rat SCaMC-3L differ from human SCaMC-3L, a predicted longer protein of 370 amino acids. In mouse and rat *SCaMC-3L* genes, the novel exon 1 displays a very short coding part covering only 6 amino acids whereas the hypothetical human *SCaMC-3L* exhibits a long exon 1 which encodes an N-terminal extension of 60 amino acids not found in murine orthologues. The existence of transcripts of human *SCaMC-3L* is supported by several EST clones and sequenced cDNA fragments. Predicted SCaMC-3L orthologues in other non-rodent mammals as chimpanzee, dog, cow or bat are also longer than murine ones, around 370-amino acids in length, harbouring conserved N-terminal extensions (Fig. 1E). These N-terminal extensions possess proline-rich sequences, containing the core PxxP (showed in Fig.1E), a structural domain not described previously in any MC, which matches consensus sequences that interact with SH3 domains [32]. Its high conservation in non-rodent mammals also suggests that SCaMC-3L exon 1 has been shortened exclusively in the rodent lineage. In agreement with that, we detected that sequences flanking the start codon are conserved between mouse and human, but those downstream, encompassing poly-proline rich region, have been replaced by a repetitive element which belongs to the short interspersed element (SINE) family (not shown). Therefore, it is likely that the insertion of this repetitive element favoured the partial lost of exon 1 sequences in mouse *SCaMC-3L*.

Despite these differences at N-termini, murine and human SCaMC-3L proteins exhibit high similarity with each other, 92 %, as well as with the carboxyl-domain of SCaMC-3 their closest paralog, around 76 %, and with the more distant paralogues SCaMC-1 and SCaMC-2, 71 %. When alignment between common regions of SCaMC-3 and SCaMC-3L counterparts was performed, we observed that substitutions are scattered along SCaMC-3L, albeit a slightly greater conservation is found in the transmembrane helixes H1, H2, H3 and H4 and in the long h_{3-4} matrix loop (see Fig. 2A). On the other hand, amino acids substitutions appear more frequently in the short external loop that connects transmembrane helixes H2-H3 and in the carboxyl-end region comprising amino acids 200 to 312. Interestingly, these residues are well conserved between SCaMC-3L orthologues. Also, three single amino acid deletions conserved in all SCaMC-3L orthologues are observed. These single deletions are not derived from intron/exon boundaries sequences and lie outside of transmembrane helixes. In addition, none of the substitutions affects residues proposed as substrate contact points for the yeast ATP-Mg/Pi carrier, Sal1p [33, 34]. According to the proposed model, Sal1p binds the adenine group to residues G416 and I417 (equivalent to G188 and I189 in SCaMC-3L, contact point II), the phosphate groups form salt bridges with residues K314 and K523 (K95 and K286 in SCaMC-3L, contact points I and III, respectively) and R242 (equivalent to R44 in SCaMC-3L) in the H1 helix, and an additional residue in contact point I, E318 (E99 in SCaMC-3L), is involved in the coordination of Mg^{2+} (Fig. 2B). Although R242 in Sal1p has not been reported to make contact points, molecular simulations and mutagenesis approaches indicate that it participates in adenine nucleotides

translocation [35, 36]. In the yeast ADP/ATP carrier Aac2p, mutation of K38, equivalent to residue R242, abolishes its transport activity [35]. These interacting residues are conserved in all human ATP-Mg/Pi carrier paralogues identified until now (not shown) [33, 34]. In particular, mouse SCaMC-3L, such as its human and rat orthologues, conserves, as previously reported [25], equivalent residues to R242 (R44), and contact points I (K95 and E99), II (G188 and I189), and III (K286) (boxed in Fig. 2A), suggesting that it could also perform an ATP-Mg/Pi counter-exchange [13, 25, 26, 27].

SCaMC-3L is a Ca^{2+}-independent ATP-Mg/Pi carrier

Although the high similarity of SCaMC-3L with other SCaMC paralogues suggested that this novel carrier probably carries out ATP-Mg/Pi exchange [25], its transport activity had not been tested to date. With this purpose, we have employed yeast expressing luciferase targeted to the mitochodrial matrix as read out system for matrix ATP levels [27]. The transport activity of SCaMC-3L was studied after expressing mouse *SCaMC-3L* in a yeast strain deficient in Sal1p [26, 27]. ATP transport in mitochondria isolated from this SCaMC-3L expressing strain was tested with a system allowing the direct quantification of mitochondrial ATP import as recently described [27].

Figure 3A, shows that *SCaMC-3L* expressing mitochondria are able to take up ATP in the presence of 20 μM carboxyatractyloside (CAT), an inhibitor of the ADP/ATP carriers, when ATP is added to the incubation medium, as shown by an increase in mitochondrial luminescence. This ATP transport activity is not present in mitochondria from the parental strain (*sal1Δ* mutant) (Fig. 3A). ATP transport by SCaMC-3L is reduced by decreasing the Mg^{2+} concentration (Fig. 3B), and also by addition of 1 mM EDTA (see below), in agreement with the fact that ATP-Mg is the transported species in mammalian and yeast ATP-Mg/Pi carriers [13, 15, 27]. ATP transport depended on the presence of phosphate in mitochondria and was reduced when the phosphate concentration was lowered, as also shown for Sal1p (results not shown, [27]). We have found that SCaMC-3L is also an ADP transporter, as shown for other mammalian and yeast mitochondrial ATP-Mg/Pi carriers [13, 15, 27]. Fig. 3C shows the increase in mitochondrial ATP obtained after ADP addition to mitochondria in the presence of CAT which follows its conversion into ATP by the H^+-ATP synthase. It is not present in the parental strain (*sal1Δ* mutant) (Fig. 3C). The rise in mitochondrial ATP after ADP addition was blocked by oligomycin, an inhibitor of the H^+-ATP synthase, as also shown for ADP uptake by Sal1p (results not shown, [27]). ADP transport was, unlike ATP transport, insensitive to 1 mM EDTA addition (Fig. 3D), in agreement with the fact that free ADP (and not ADP-Mg) is the transported species in other ATP-Mg/Pi carriers [13, 15, 27].

The kinetics of ATP and ADP influx along SCaMC-3L over a range of external concentrations of ATP and ADP is shown in Fig. 3E. The apparent K_M for ATP was 0.41 +/- 0.08 mM (mean +/- SEM of 3 independent experiments performed in duplicate), similar to that obtained previously for a truncated version of human SCaMC-3, containing only the mitochondrial carrier homology region, and reconstituted in proteoliposomes (0.22 mM) [13], confirming as well that the N-extension is not required for its transport function. It was also similar to that of Sal1p in yeast mitochondria (0.20-0.24 mM) [27]. For ADP the K_M,

0.90 +/- 0.12 mM (mean +/- SEM of 3 independent experiments performed in duplicate), was higher than that for ATP, as also shown for SCaMC-3 (0.54 mM) [27], and unlike Sal1p and SCaMC-1 which have similar K_M for ATP and ADP [13, 27]. On the other hand, the V_{MAX} for ATP and ADP transport through SCaMC-3L was similar, as for the other ATP-Mg/Pi carriers studied so far [13, 27]. Significantly, as expected from its lack of calcium binding domains, metabolite transport mediated by SCaMC-3L was calcium-insensitive, in contrast with the behaviour of Sal1p, the only representative of the ATP-Mg/Pi carriers whose Ca^{2+}-regulation has been studied (Fig. S1). In sum, our results prove that SCaMC-3L is a true mitochondrial transporter of ATP-Mg/Pi which, unlike its other paralogues, is Ca^{2+}-independent.

The tandem duplication event of the *SCaMC-3* ancestor occurred prior to mammalian radiation

To date three ATP-Mg/Pi paralogues, SCaMC-1, -2 and -3, have been described in vertebrates genomes. All are probably generated by gene duplication events, the major source of new genes in vertebrates [37]. As a number of insects, see urchin or *Ciona intestinalis*, a basal chordate and representative of outgroup to the vertebrates, all present a single *SCaMC* counterpart, it is reasonable to consider that the ATP-Mg/Pi paralogues arose during large-scale genome-amplification events that occurred around the time of origin of vertebrates [38]. In fact, human *SCaMCs* map at chromosomal loci enclosed in regions belonging to the characterised major histocompatibility complex (MHC) paralogous region 6p/1p/9q/19p [12, 39, 40]. Analysis of these regions in human and amphioxus supports that MHC-paralogous regions are the result of *en bloc* duplications that occurred after the divergence of cephalochordates and vertebrates (around 750 Myr ago, [40, 41]). However, BLASTN searches using mouse *SCaMC-3L* as query failed to detect *SCaMC-3L* ortholog sequences in either fish, amphibian or bird genomes, suggesting that this carrier may represent a more recent acquisition exclusive of mammalian genomes.

Thus, an interesting question was whether its apparition was linked to the initial mammalian radiation or represented a more recent event. With this purpose, we searched for *SCaMC-3L and SCaMC-3* orthologues in relevant mammalian and vertebrate genomes currently available to ascertain its phylogenetic relationships. The high conservation degree within each *SCaMC* subgroup facilitates the identification of orthologues, as opposed to paralogues, among species by reciprocal-best-blast tests. In addition, all *SCaMC-3/SCaMC-3L* loci analysed display an identical head-to-tail arrangement favouring their identification. *SCaMC-3* orthologues are found in pufferfish (*Tetraodon nigroviridis*) and zebrafish (*Danio rerio*) and, although no *SCaMC-3* counterparts are detected in frogs or chicken, highly conserved *SCaMC-3* counterparts are detected in all mammals analysed including the monotreme platypus (*Ornithorhynchus anatinus*). In chicken, the homologous segment to human region encompassing the SCaMC-3 locus has been lost in the corresponding synteny block on chicken chromosome 28 [42]. On the other hand, we have identified *SCaMC-3L* orthologues in all placental mammals with available genomes, as well as in the marsupial opossum (*Monodelphis domestica*), but not in platypus. In the platypus genome, a large genomic clone containing *SCaMC-3* without adjacent *SCaMC-3L*-related sequences has been detected (accession number AAPN01306014). This suggests that duplication of the *SCaMC-3L* ancestor could have occurred in

mammals after radiation from monotremes. This hypothesis was tested constructing a phylogenetic tree with representative SCaMC-3 and SCaMC-3L proteins using the neighbour-joining method (Phylo_win, [29]) and with non-vertebrates SCaMCs as basal outgroup. As is shown in Fig. 4, the topology of the tree clearly rules out that the ancestral *SCaMC-3* duplication occurred in monotremes. SCaMC-3L and SCaMC-3 mammalian orthologues (including platypus counterpart) form two independent and well defined clades and it is likely that the partial duplication event that generated the SCaMC-3L paralog occurred prior to the mammalian radiation (80-430 Myr ago, [41]), probably after divergence between fish and tetrapod lineages, by means of a small-scale tandem duplication not related to large scale duplications common of vertebrates. Unfortunately, the lack of SCaMC-3 counterparts in amphibians and birds prevents to determine with more precision when *SCaMC-3L* subfamily emerged. Nevertheless, its maintenance in all mammalian groups indicates that SCaMC-3L plays a relevant function in this lineage.

Interestingly, although we detected high homology among SCaMC-3L paralogues, the SCaMC-3L cluster shows a branch longer than that of SCaMC-3, suggesting unequal evolution between paralogues. It is possible that the partial duplication created a non-functional product that underwent an accelerated rate of amino-acid changes during the period following gene duplication. Later, the duplicated gene became functional by the acquisition of a novel first exon and cis-regulatory elements, resulting, finally, in a relatively distant subfamily whose members have evolved maintaining high homology inside the cluster (see alignment in fig. S2).

SCaMC-3L expression is restricted to testis and brain

It has been hypothesized that duplicated versions would be evolutionary retained if they diverge acquiring novel functions or if original functions are subdivided between ancestral and newly duplicated version [43-47]. Indeed, a common fate postulated for the members of duplicated-gene pairs is the partitioning of tissue-specific expression patterns of the ancestral gene [43, 44]. In order to compare expression patterns between duplicates, we analysed their distribution in mouse tissues by RT-PCR (Fig. 5) and northern analysis (Fig. S3), confirming that *SCaMC-3* and *SCaMC-3L* display non-coincident expression patterns. In mouse tissues, *SCaMC-3L* expression is mainly detected in testis and, in lesser levels, in brain (Fig. 5) whereas that *SCaMC-3* is broadly distributed in most tissues, including testis and brain (Fig 5), as previously reported [12, 13, 24]. A similar expression pattern is also detected for *SCaMC-3L* in rat tissues (Fig. 5, bottom panel). Although, it has been previously reported that in rat *SCaMC-3L* is expressed mainly in brain and at low levels in testis [25], the observed testis-predominant pattern matches well with the origin of mouse *SCaMC-3L* EST-clones found in databases where 8 out 10 derived from testis (NCBI Unigene Mm.33647). Moreover, mouse *SCaMC-3L* transcript harbours a short 3'UTR, a common feature of testis-specific transcripts. In contrast, in other non-rodent mammals as human or cow, *SCaMC-3L*-clones derive principally from brain and liver indicating that *SCaMC-3L* is differentially expressed among mammalian subgroups but always shows a more limited expression pattern than *SCaMC-3*.

SCaMC-3L represents, therefore, a clear example of gene duplication followed by subfunctionalization which takes place both at structural and expression levels. On the structural level, SCaMCs are proteins with two separated functional modules; this aspect makes them prone to subfunctionalization since it facilitates that newly duplicated copies undergo independent changes in each module to carry out only a fraction of the original functions [45, 47]. The duplication event that generated SCaMC-3L was partial, as found for 50 % of newborn duplications in *C. elegans* [48], and the exons of the ancestral gene encoding calcium-binding domains were not included in the duplicated segment. Thus, in SCaMC-3L the entire regulatory calcium-binding N-extension distinctive of SCaMC members has been lost, maintaining intact the transport module. A second mechanism of subfunctionalization at the expression level is based on the divergence and subdivision of the cis-regulatory elements of the parental gene, so that the newly duplicated gene has a more restricted distribution, probably in a subset of the tissues where its ancestors were distributed [38, 40, 41, 43]. In mouse and rat tissues, *SCaMC-3L* expression is mainly detected in testis whereas *SCaMC-3* is expressed in most tissues. This predominant testis-expression is infrequent among MCF genes. A notable exception is the ADP/ATP translocases, where a newly discovered fourth member AAC4/slc25a31, is expressed exclusively in testis [10, 49, 50] and has been found essential for spermatogenesis [10]. In addition, SCaMC-1a, a SCaMC-1 isoform found in primates, is expressed from a testis-specific promoter [13, 17]. Collectively, these results suggest that mitochondrial transport of adenine nucleotides by either the testis specific ADP/ATP carriers that are classically involved in oxidative phosphorylation or the testis-specific ATP-Mg/Pi carriers that catalyze a net accumulation or depletion of mitochondrial adenine nucleotides is important in testicular development or spermatogenesis. The specific role of each of these transporters, and, particularly, the two ATP-Mg/Pi carriers enriched in primate testis, the Ca^{2+}-dependent SCaMC-1a and the Ca^{2+}-independent SCaMC-3L remains to be established.

Acknowledgements: This work was supported by grants from Ministerio de Educación y Ciencia (BFU2005-C02-01, GEN2003-20235-C05-03/NAC), European Union (LSHM-CT-2006-518153), Comunidad de Madrid (S-GEN-0269-2006 MITOLAB-CM) and CIBER de Enfermedades Raras an initiative of the ISCIII, and by an institutional grant from the Fundación Ramón Areces to the Centro de Biología Molecular Severo Ochoa. JT was a recipient of a FPU fellowship from the Ministerio de Educación y Ciencia.

REFERENCES

1. Palmieri, F. (2004) The mitochondrial transporter family (SLC25): physiological and pathological implications. Pflugers Arch. **447**, 689-709

2. Kunji, E. R. (2004) The role and structure of mitochondrial carriers. FEBS Lett. **564**, 239-44

3. del Arco A and Satrústegui J. (2005) New mitochondrial carriers: an overview. Cell. Mol. Life Sci. **62**, 2204-27.

4. Pebay-Peyroula, E., Dahout-Gonzalez, C., Kahn, R., Trézéguet, V., Lauquin, G.J. and Brandolin, G. (2003) Structure of mitochondrial ADP/ATP carrier in complex with carboxyatractyloside. Nature **426**, 39-44

5. Nelson, D. R., Felix, C. M. and Swanson, J. M. (1998) Highly conserved charge-pair networks in the mitochondrial carrier family. J. Mol. Biol. **277**, 285-308

6. Picault, N., Hodges, M., Palmieri, L. and Palmieri F. (2004) The growing family of mitochondrial carriers in Arabidopsis. Trends Plant Sci. **9**, 138-46

7. Millar, A.H. and Heazlewood, J.L. (2003) Genomic and proteomic analysis of mitochondrial carrier proteins in Arabidopsis. Plant Physiol. **131**, 443-53

8. Satre, M., Mattei, S., Aubry, L., Gaudet, P., Pelosi, L., Brandolin, G. and Klein, G. (2007) Mitochondrial carrier family: repertoire and peculiarities of the cellular slime mould *Dictyostelium discoideum*. Biochimie **89**, 1058-69

9. el Moualij, B., Duyckaerts, C., Lamotte-Brasseur, J., Sluse, F.E. (1997) Phylogenetic classification of the mitochondrial carrier family of Saccharomyces cerevisiae. Yeast 13, 573-81.

10. Brower, J.V., Rodic, N., Seki, T., Jorgensen, M., Fliess, N., Yachnis, A.T., McCarrey, J.R., Oh, S.P. and Terada, N. (2007) Evolutionarily conserved mammalian adenine nucleotide translocase 4 is essential for spermatogenesis. J. Biol. Chem. **282**, 29658-66

11. Palmieri, L., Picault, N., Arrigoni, R., Besin, E., Palmieri, F. and Hodges, M. (2008) Molecular identification of three Arabidopsis thaliana mitochondrial dicarboxylate carrier isoforms: organ distribution, bacterial expression, reconstitution into liposomes and functional characterization. Biochem. J. **410**, 621-9

12. del Arco, A. and Satrustegui, J. (2004) Identification of a novel human subfamily of mitochondrial carriers with calcium-binding domains. J. Biol. Chem. **279**, 24701-13

13. Fiermonte, G., De Leonardis, F., Todisco, S., Palmieri, L., Lasorsa, F. M., Palmieri, F. (2004) Identification of the mitochondrial ATP-Mg/Pi transporter. Bacterial expression, reconstitution, functional characterization, and tissue distribution. J. Biol. Chem. **279**, 30722-30

14. Aprille, J. R. (1988) Regulation of the mitochondrial adenine nucleotide pool size in liver: mechanism and metabolic role. FASEB J. **2**, 2547-56

15. Aprille JR. (1993) Mechanism and regulation of the mitochondrial ATP-Mg/P(i) carrier. J. Bioenerg. Biomembr. **25**, 473-81

16. Joyal, J. L. and Aprille, J. R. (1992) The ATP-Mg/Pi carrier of rat liver mitochondria catalyzes a divalent electroneutral exchange. J. Biol. Chem. **267**, 19198-203

17. Satrústegui, J., Pardo, B. and del Arco A. (2007) Mitochondrial transporters as novel targets for intracellular calcium signaling. Physiol. Rev. **87**, 29-67

18. del Arco, A. and Satrústegui, J. (1998) Molecular cloning of Aralar, a new member of the mitochondrial carrier superfamily that binds calcium and is present in human muscle and brain. J. Biol. Chem. **273**, 23327-34

19. del Arco, A., Agudo, M. and Satrústegui, J. (2000) Characterization of a second member of the subfamily of calcium-binding mitochondrial carriers expressed in human non-excitable tissues. Biochem. J. **345**, 725-32

20. Palmieri, L., Pardo, B., Lasorsa, F. M., del Arco, A., Kobayashi, K., Iijima, M., Runswick, M. J., Walker, J. E., Saheki, T., Satrustegui, J. and Palmieri, F. (2001) Citrin and aralar1 are Ca(2+)-stimulated aspartate/glutamate transporters in mitochondria. EMBO J. **20**, 5060-9

21. Lasorsa, F.M., Pinton, P., Palmieri, L., Fiermonte, G., Rizzuto, R. and Palmieri, F. (2003) Recombinant expression of the Ca(2+)-sensitive aspartate/glutamate carrier increases mitochondrial ATP production in agonist-stimulated Chinese hamster ovary cells. J. Biol. Chem. **278**, 38686-92

22. Pardo, B., Contreras, L., Serrano, A., Ramos, M., Kobayashi, K., Iijima, M., Saheki, T. and Satrústegui, J. (2006) Essential role of aralar in the transduction of small Ca2+ signals to neuronal mitochondria. J. Biol. Chem. **281**, 1039-47

23. Contreras, L., Gomez-Puertas, P., Iijima, M., Kobayashi, K., Saheki, T. and Satrústegui J. (2007) Ca2+ Activation kinetics of the two aspartate-glutamate mitochondrial carriers, aralar and citrin: role in the heart malate-aspartate NADH shuttle. J. Biol. Chem. **282**, 7098-106

24. del Arco, A. (2005) Novel variants of human SCaMC-3, an isoform of the ATP-Mg/P(i) mitochondrial carrier, generated by alternative splicing from 3'-flanking transposable elements. Biochem. J. **389**, 647-55

25. Haitina, T., Lindblom, J., Renstrom, T. and Fredriksson, R. (2006) Fourteen novel human members of mitochondrial solute carrier family 25 (SLC25) widely expressed in the central nervous system. Genomics **88**, 779-90

26. Cavero, S., Traba, J., del Arco, A. and Satrústegui, J. (2005) The calcium-dependent ATP-Mg/Pi mitochondrial carrier is a target of glucose-induced calcium signalling in *Saccharomyces cerevisiae*. Biochem. J. **392**, 537-44

27. Traba, J., Froschauer, E., Wiesenberger, G., Satrústegui, J. and del Arco, A. (2008) Yeast mitochondria import ATP through the calcium-dependent ATP-Mg/Pi carrier Sal1p, and are ATP consumers during aerobic growth in glucose. Mol. Microbiol. **69**, 570-85

28. Kucejova B, Li L, Wang X, Giannattasio S, Chen XJ. (2008) Pleiotropic effects of the yeast Sal1 and Aac2 carriers on mitochondrial function via an activity distinct from adenine nucleotide transport. Mol Genet Genomics **280**, 25-39

29. Galtier, N., Gouy, M. and Gautier, C. (1996) SeaView and Phylo_win, two graphic tools for sequence alignment and molecular phylogeny. Comput. Applic. Biosci. **12**, 543-548

30. Zúñiga, S., Boskovic, J., Jiménez, A., Ballesta, J.P. and Remacha, M. (1999) Disruption of six *Saccharomyces cerevisiae* novel genes and phenotypic analysis of the deletants. Yeast. **15**, 945-53

31. Arechaga, I., Raimbault, S., Prieto, S., Levi-Meyrueis, C., Zaragoza, P., Miroux, B., Ricquier, D., Bouillaud, F. and Rial, E. (1993) Cysteine residues are not essential for uncoupling protein function. Biochem. J. **296**, 693-700

32. Kay, B.K., Williamson, M.P. and Sudol, M. (2000) The importance of being proline: the interaction of proline-rich motifs in signaling proteins with their cognate domains. FASEB J. **14**, 231-41

33. Kunji, E.R. and Robinson, AJ (2006) The conserved substrate binding site of mitochondrial carriers. Biochim. Biophys. Acta **1757**, 1237-48

34. Robinson, A.J. and Kunji, E.R. (2006) Mitochondrial carriers in the cytoplasmic state have a common substrate binding site. Proc Natl Acad Sci U S A. **103**, 2617-22

35. Müller, V., Heidkämper, D., Nelson D.R. AND Klingenberg, M. (1997) Mutagenesis of some positive and negative residues occurring in repeat triad residues in the ADP/ATP carrier from yeast. Biochemistry, **36**, 16008-18.

36. Wang, Y. and Tajkhorshid, E. (2008) Electrostatic funneling of substrate in mitochondrial inner membrane carriers. Proc Natl Acad Sci U S A. **105**, 9598-603.

37. Ohno, S. Evolution by gene duplication (Springer, New York, 1970)

38. McLysaght, A., Hokamp, K. and Wolfe, KH. (2002) Extensive genomic duplication during early chordate evolution. Nat. Genet. **31**, 200-48

39. Kasahara, M., Nakaya, J., Satta, Y. and Takahata, N. (1997) Chromosomal duplication and the emergence of the adaptive immune system. Trends Genet. **13**, 90-2

40. Abi-Rached, L., Gilles, A., Shiina, T., Pontarotti, P. and Inoko H. (2002) Evidence of en bloc duplication in vertebrate genomes. Nat. Genet. **31**, 100-5

41. Gu, X., Wang, Y. and Gu, J. (2002) Age distribution of human gene families shows significant roles of both large- and small-scale duplications in vertebrate evolution. Nat. Genet. **31**, 205-9

42. Gordon, L., Yang, S., Tran-Gyamfi, M., Baggott, D., Christensen, M., Hamilton, A., Crooijmans, R., Groenen, M., Lucas, S., Ovcharenko, I. and Stubbs, L. (2007) Comparative analysis of chicken chromosome 28 provides new clues to the evolutionary fragility of gene-rich vertebrate regions. Genome Res. **17**, 1603-13

43. Force, A., Lynch, M., Pickett, F.B., Amores, A., Yan, Y.L. and Postlethwait J. (1999) Preservation of duplicate genes by complementary, degenerative mutations. Genetics **151**, 1531-45

44. Lynch, M. and Force, A. (2000) The probability of duplicate gene preservation by subfunctionalization. Genetics **154**, 459-73

45. Louis, E.J. (2007) Evolutionary genetics: making the most of redundancy. Nature **449**, 673-4

46. Hurles M. (2004) Gene duplication: the genomic trade in spare parts. PLoS Biol. **2**, E206

47. Hittinger, C.T. and Carroll, S.B. (2007) Gene duplication and the adaptive evolution of a classic genetic switch. Nature **449**, 677-81

48. Katju, V. and Lynch, M. (2006) On the formation of novel genes by duplication in the *Caenorhabditis elegans* genome. Mol. Biol. Evol. **23**, 1056-67

49. Dolce, V., Scarcia, P., Iacopetta, D. and Palmieri, F. (2005) A fourth ADP/ATP carrier isoform in man: identification, bacterial expression, functional characterization and tissue distribution. FEBS Lett. **579**, 633-7

50. Kim, Y.H., Haidl, G., Schaefer, M., Egner, U., Mandal, A. and Herr, J.C. (2007) Compartmentalization of a unique ADP/ATP carrier protein SFEC (Sperm Flagellar Energy Carrier, AAC4) with glycolytic enzymes in the fibrous sheath of the human sperm flagellar principal piece. Dev. Biol. **302**, 463-76

FIGURE LEGENDS

Fig. 1 *SCaMC-3L* a novel shortened SCaMC paralog generated by a tandem partial duplication of *SCaMC-3* (A) Scheme of *SCaMC-3(Slc25a23)/SCaMC-3L*(*Slc25a41*) genomic organization in mouse. Exons are represented as numbered filled boxes and non-translated sequences are indicated as open boxes. SCaMC-3L exon 1, unrelated to SCaMC-3 sequences, is shown as striped box. Exons are not drawn to scale. Amino acids identities of *SCaMC-3L* exons respect to their corresponding *SCaMC-3* exons are indicated in percentage. Identical genomic structure and head-to-tail tandem array are found for all mammalian *SCaMC-3/SCaMC-3L* loci analysed. Its structure and conservation degree suggest that *SCaMC-3L* evolved from an ancestral *SCaMC-3* by a partial duplication. **(B)** Diagram of the structure of mouse SCaMC-3 and SCaMC-3L proteins. Mitochondrial Carrier (MC) homology region and the EF-hands calcium-binding domains of SCaMC-3 are indicated.

(C, D) SCaMC-3L resides in mitochondria. Immunofluorescence assays of COS-7 cells transiently transfected with carboxyl-FLAG-tagged SCaMC-3L, SCaMC-3L$_{FLAG,}$ and stained with MitoTracker or co-transfected with DsRed2-Mito as mitochondrial control. SCaMC-3 L$_{FLAG}$ was detected using an anti-FLAG antibody and visualized with FITC secondary antibody. Anti-FLAG staining totally match with that of mitochondrial markers used. Magnification x63; scale bars 10 µm. Western blot analysis of total homogenate (H) mitochondria-enriched fraction (Mit) and post-mitochondrial supernatant (PM) (10 µg per lane) from HEK-293T cells transfected with SCaMC-3L$_{FLAG}$. Membrane was immunoblotted with anti-FLAG antibody. As control of mitochondrial purification anti-SCaMC-1 was used. The position of molecular mass marker is indicated.

(E) Comparison of SCaMC-3L sequences non-derived from SCaMC-3. Multiple alignment of predicted sequences corresponding to SCaMC-3L exon 1 and firsts amino acids belonging to exon 2 from representative species was performed with Clustalw and coloured using Boxshade program. Non-rodents species exhibit a conserved N-terminal extension derived from exon 1 sequences which is absent in rodent SCaMC-3L orthologues. The accession numbers of sequences used are indicated in parenthesis; *Mus musculus* (NP_780542); *Rattus novergicus* (XP_001059741); *Homo sapiens* (NP_775908); *Pan troglodytes* (XP_524070.2); *Canis familiaris* (XP_542139.1); *Bos taurus* (NP_001069309) and *Myotis lucifugus* (AAPE01371874.1). Poly-proline stretches present in non-rodent SCaMC-3L are underlined.

Fig. 2 SCaMC-3L and SCaMC-3 paralogues show high homology at the MC domain and conserve substrate contact points for ATP-Mg and Pi (A) Alignment of the MC domain of mouse, rat and human SCaMC-3L with that of SCaMC-3 consensus. Alignment of SCaMC-3 sequences encoded by exons 5 to 10 of human, chimp, rhesus, mouse and rat SCaMC-3 orthologues was performed with ClustalW program and the consensus sequence was obtained with BOXSHADE 3.21 program. A multiple alignment including sequences corresponding to exons 2 to 7 of SCaMC-3L orthologues and SCaMC-3 consensus was also

performed with the ClustalW program and is also shown. Dots represent conserved residues and dashes insertions. Secondary structure prediction for mouse SCaMC-3L obtained using APSSP server is showed (*H*, helix; *E*, strand; *C*, coil). The transmembrane helixes are indicated and numbered, in lower case letter are marked the helixes of the matrix loops. SCaMCs residues proposed as participants in substrate interactions placed in even transmembranes [33, 34] are included in red boxes and R44, an additional residue involved in phosphate groups interaction [33, 34], is indicated with asterisk.

(B) Model of SCaMC-3L viewed from the mitochondrial intermembrane space. Only the transmembrane helixes (H1 to H6 are shown). ATP-Mg is bound to contact points I, II, and III and an additional residue, R44, equivalent to K22 of BtAAC1, in helix 1 [33, 34]. Mg^{2+} is depicted as a sphere. The adenine group binds contact point II (helix 4) through hydrophobic interactions with G188 and I189, while the phosphate groups bind contact points I (helix 2) and III (helix 6) through interactions with K95 and K286, respectively, and R44. E99, at contact point I, is involved in the coordination of Mg^{2+}. The model was generated by the Phyre web server using the adenine nucleotide translocase as a template and using contact points equivalent to those described for Sal1p [33, 34].

Fig. 3 Transport activity of SCaMC-3L (A) Mitochondria of *sal1Δ* cells expressing luciferase from plasmid pYeDP-Cox4-Luc and *SCaMC-3L* from plasmid pYX142 were incubated with 5 mM succinate as respiratory substrate, 2 mM Na_2HPO_4, 5 mM $MgCl_2$ and 0.1 mM luciferin in the presence of 20 μM CAT. Mitochondria of *sal1Δ* cells expressing luciferase were shown as a control (grey trace). Free Ca^{2+} was around 15 μM. ATP (0.5 mM) was added at the arrowhead. Luminescence was measured every 10 seconds and was transformed to ATP concentration using the calibration curves [27]. A representative experiment for each strain is shown. **(B)** Mitochondria of the same cells were incubated as indicated above except that the $MgCl_2$ concentration was varied as indicated. **(C)** Mitochondria of the same cells were incubated as indicated above except that 1 mM ADP was added at the arrowhead. Mitochondria of *sal1Δ* cells expressing luciferase were shown as a control (grey trace). **(D)** Mitochondria of the same cells were incubated as indicated above except that the $MgCl_2$ concentration was varied by addition of 0 (black traces) or 1 mM EDTA (grey traces), and 1 mM ATP or ADP were added at the arrowhead. **(E)** The rates of ATP and ADP transport (closed and open squares respectively) through SCaMC-3L were studied in mitochondria of the same cells after the addition of different ATP and ADP concentrations. The transport rates are expressed relative to the maximum rate obtained with saturating ATP. The data were fit by nonlinear regression to the equation: $V = (V_{max} \times [\text{nucleotide}]) / (K_m + [\text{nucleotide}])$ (where V is the transport activity obtained at each [nucleotide], V_{max} is the maximal activity and K_m is the nucleotide concentration which generates half-maximal transport activity). Data are mean ± SEM of three independent experiments performed in duplicate.

Fig. 4. Phylogenetic relationship between SCaMC-3 and SCaMC-3L paralogues

The phylogenetic tree has been constructed using Phylo_win program [29] with neighbour-joining method and PAM distances. Non-vertebrates SCaMCs were used as outgroups. The scale of branch lengths is indicated (number of substitutions per site). Percentage bootstrap values are shown in each node (500 replicates). The GenBank™ accession numbers of the protein sequences are indicated in parentheses: See urchin (XP_001201883); *Drosophila melanogaster* (NP_729802); Pufferfish (CAG06041*); Zebrafish (XP_690428); Human_3 (NP_077008); Chimp_3 (XP_524071*); Rhesus_3 (XP_001088378); Mouse_3 (NP_080153); Rat_3 (NP_001100343); Dog_3 (XP_542138); Cow_3 (XP_001253949*); Opossum_3 (XP_001376701); Platypus_3 (XP_001519699); Human_3L (NP_775908); Chimp_3L (XP_524070); Rhesus_3L (XM_001091089*); Mouse_3L (NP_780542); Rat_3L (NP_001100344); Dog_3L (XP_542139); Cow_3L (NP_001069309*); Opossum _3L (XP_001376688). Amino acids sequences from entries mark with asterisks have been partially corrected according to genomic sequences.

Fig. 5. Murine *SCaMC-3L* and *SCaMC-3* show different expression pattern

RT-PCR analysis for *SCaMC-3L* and *SCaMC-3* expression in different mouse tissues (upper panels) and for *SCaMC-3L* in rat tissues (bottom panels). Equivalent aliquots of cDNAs derived from the indicated tissues were used as templates. Amplification of β-actin was used as an internal control. Unspecific liver band is indicated with asterisk. The results obtained indicate that *SCaMC-3/SCaMC-3L* are differently expressed displaying *SCaMC-3L* a testis-predominant pattern.

Biochemical Journal Immediate Publication. Published on 17 Oct 2008 as manuscript BJ20081262

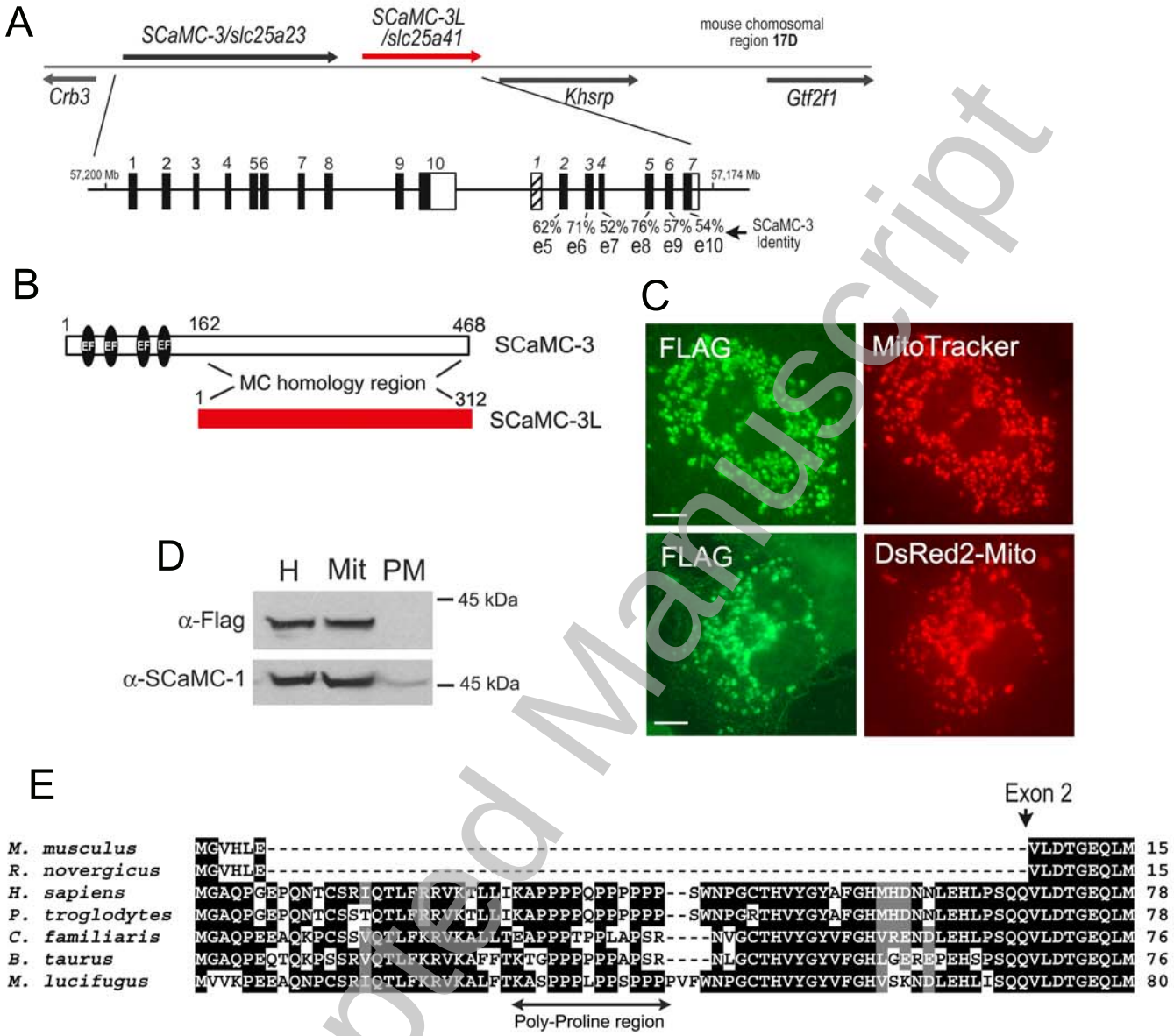

Figure 1

Figure 2

Biochemical Journal Immediate Publication. Published on 17 Oct 2008 as manuscript BJ20081262

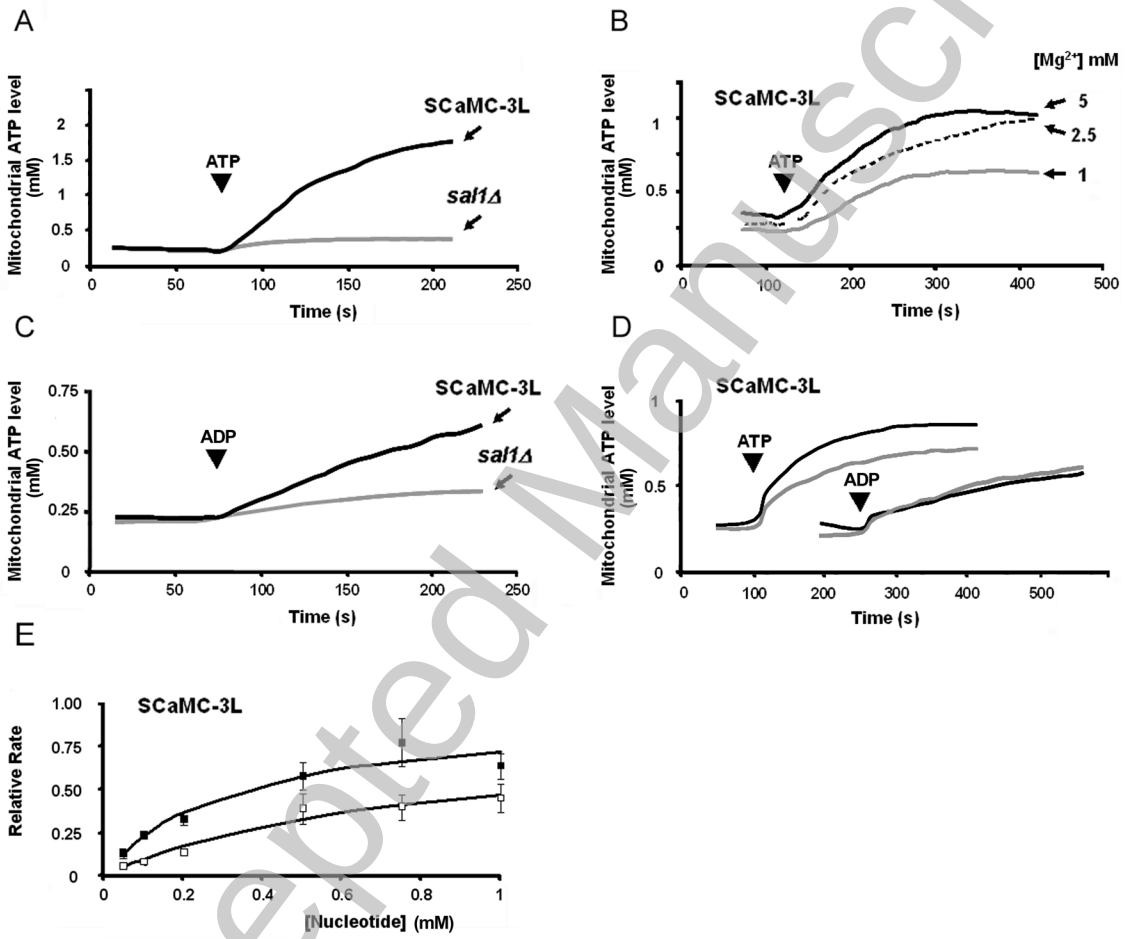

Figure 3

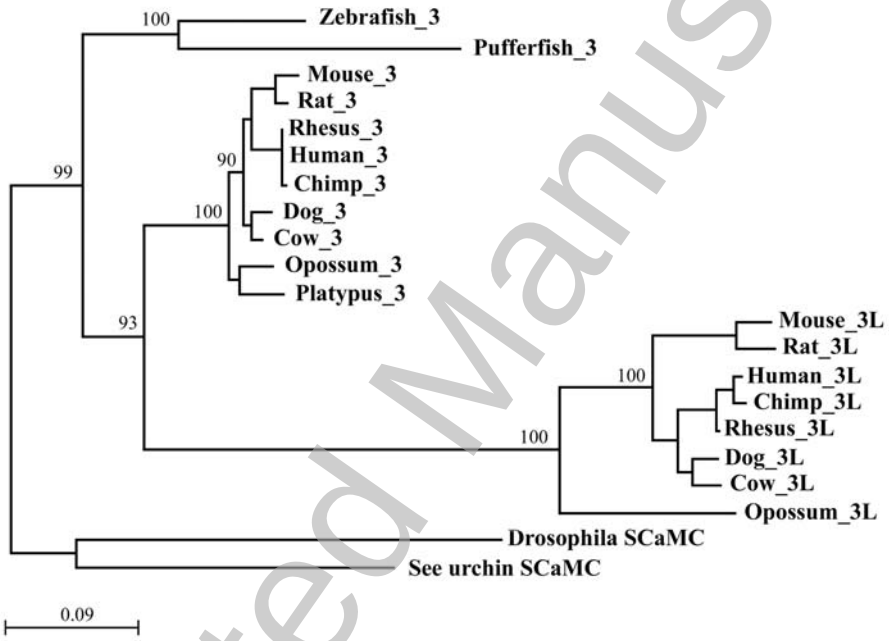

Figure 4

Biochemical Journal Immediate Publication. Published on 17 Oct 2008 as manuscript BJ20081262

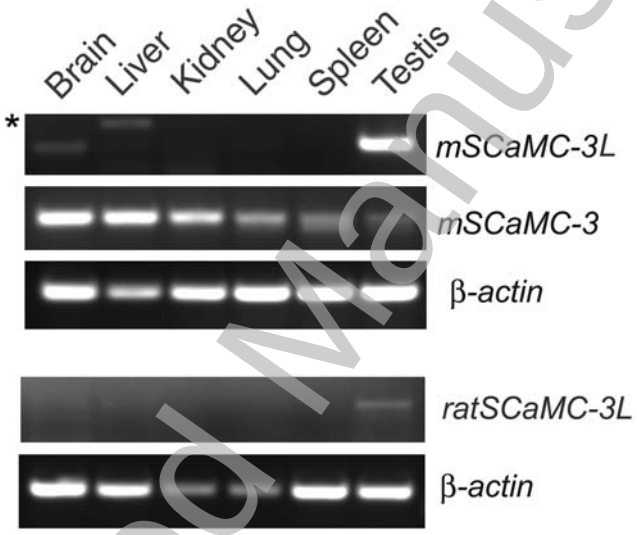

Figure 5